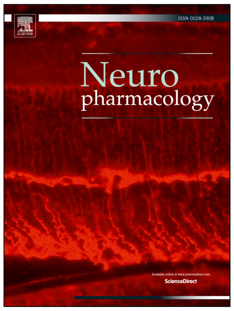

Inhibition of cathepsin X reduces the strength of microglial-mediated neuroinflammation

Anja Pišlar, Biljana Božić, Nace Zidar, Janko Kos

PII: S0028-3908(16)30523-8
DOI: 10.1016/j.neuropharm.2016.11.019
Reference: NP 6515

To appear in: *Neuropharmacology*

Received Date: 28 June 2016
Revised Date: 8 October 2016
Accepted Date: 22 November 2016

Please cite this article as: Pišlar, A., Božić, B., Zidar, N., Kos, J., Inhibition of cathepsin X reduces the strength of microglial-mediated neuroinflammation, *Neuropharmacology* (2016), doi: 10.1016/j.neuropharm.2016.11.019.

This is a PDF file of an unedited manuscript that has been accepted for publication. As a service to our customers we are providing this early version of the manuscript. The manuscript will undergo copyediting, typesetting, and review of the resulting proof before it is published in its final form. Please note that during the production process errors may be discovered which could affect the content, and all legal disclaimers that apply to the journal pertain.

Inhibition of cathepsin X reduces the strength of microglial-mediated neuroinflammation

Anja Pišlar[a,*], Biljana Božić[b], Nace Zidar[c] and Janko Kos[a,d]

[a]Department of Pharmaceutical Biology, Faculty of Pharmacy, University of Ljubljana, Aškerčeva 7, SI-1000 Ljubljana, Slovenia.
[b]Institute for Physiology and Biochemistry, Faculty of Biology, University of Belgrade, Studentski trg 16, 11000 Belgrade, Serbia.
[c]Department of Pharmaceutical Chemistry, Faculty of Pharmacy, University of Ljubljana, Aškerčeva 7, SI-1000 Ljubljana, Slovenia.
[d]Department of Biotechnology, Jožef Stefan Institute, Jamova cesta 39, SI-1000 Ljubljana, Slovenia.

Highlights

- *i.) Microglia activation induces cathepsin X expression and its activity.*
- *ii.) Cathepsin X inhibition suppresses microglia activation.*
- *iii.) Cathepsin X mediates microglia activation-mediated neurodegeneration.*
- *iv.) Cathepsin X inhibition exerts neuroprotection.*

Abbreviations: 6-OHDA, 6-hydroxydopamine; BSA: bovine serum albumin; CNS, central nervous system; DMEM, Dulbecco’s modified Eagle’s medium; ELISA, enzyme-linked immune sorbent assay; ERK, extracellular signal-regulated kinase; FBS, fetal bovine serum; HRP, horseradish peroxidase; IL-6, interleukin-6; JNK, Jun-N-terminal kinase; LPS, lipopolysaccharide; MAPK, mitogen-activated protein kinase; MCS, microglial culture supernatant; MTS, 3-(4,5-dimethylthiazol-2-yl)-5-(3-carboxymethoxyphenyl)-2-(4-sulfophenyl)-2H-tetrazolium, inner salt; NO, nitric oxide; PBS, phosphate buffered saline; ROS, reactive oxygen species; TNF-α, tumor necrosis factor α; γ-ENO, γ-enolase peptide.

* Corresponding author: Anja Pišlar, Faculty of Pharmacy, University of Ljubljana, Aškerčeva 7, 1000 Ljubljana, Tel: +368 1 4769526, Fax: +386 1 4258031, E-mail: anja.pislar@ffa.uni-lj.si

Abstract

Inflammation plays a central role in the processes associated with neurodegeneration. The inflammatory response is mediated by activated microglia that release inflammatory mediators to the neuronal environment. Microglia-derived lysosomal cathepsins, including cathepsin X, are increasingly recognized as important mediators of the inflammation involved in lipopolysaccharide (LPS)-induced neuroinflammation. The current study was undertaken to investigate the role of cathepsin X and its molecular target, γ-enolase, in neuroinflammation and to elucidate the underlying mechanism. We determined that the exposure of activated BV2 and EOC 13.31 cells to LPS led to increased levels of cathepsin X protein and activity in the culture supernatants in a concentration- and time-dependent manner. In contrast, LPS stimulation of these two cells reduced the release of active γ-enolase in a manner regulated by the cathepsin X activity. Cathepsin X inhibitor AMS36 significantly reduced LPS-induced production of nitric oxide, reactive oxygen species and the pro-inflammatory cytokines interleukin-6 and tumor necrosis factor-α from BV2 cells. Inhibition of cathepsin X suppressed microglial activation through the reduced caspase-3 activity, together with diminished microglial cell death and apoptosis, and also through inhibition of the activity of the mitogen-activated protein kinases. Further, SH-SY5Y treatment with culture supernatants of activated microglial cells showed that cathepsin X inhibition reduces microglia-mediated neurotoxicity. These results indicate that up-regulated expression and increased release and activity of microglial cathepsin X leads to microglia activation-mediated neurodegeneration. Cathepsin X inhibitor caused neuroprotection via its inhibition of the activation of microglia. Cathepsin X could thus be a potential therapeutic target for neuroinflammatory disorders.

Keywords: Cathepsin X, γ-Enolase, Microglia, Neuroinflammation, Neuroprotection.

1. Introduction

Microglial cells are macrophage-like cells resident in the central nervous system (CNS) that have a ramified morphology. Their proper function is required for optimal brain function and for the prevention of neuroinflammation and neurodegeneration. During loss of brain homeostasis, which is dangerous for the CNS, microglia receive signals by a number of receptors. These signals evoke rapid changes in microglial cell shape, gene expression and functional behavior, together known as “microglial activation”. Activation of microglia is the hallmark of neurodegenerative disorders associated with chronic neuroinflammation. It is characterized by increased phagocytic activity and intensive production of pro-inflammatory molecules including chemokines, cytokines, reactive oxygen species (ROS), and nitric oxide (NO) (Kettenmann et al., 2011). On the other hand, in response to neuronal injury, microglia secrete neurotrophic factors that support the remaining healthy neurons (Nakajima et al., 2001, Schindowski et al., 2008). It is now widely accepted that microglia play important roles in homeostasis and pathogenesis in the CNS (Li et al., 2007).

There is increasing evidence that activated microglia also induce the synthesis and secretion of lysosomal cathepsins (Kingham and Pocock, 2001, Nakanishi, 2003a, Wendt et al., 2009, Clark and Malcangio, 2012, Fan et al., 2012, Hafner et al., 2013, Lively and Schlichter, 2013, Fan et al., 2015). Cysteine cathepsins constitute the largest cathepsin family, including the 11 members (cathepsins B, C, F, H, K, L, O, S, W, V and X) that possess a conserved active site involving cysteine, histidine and asparagine residues in the catalytic triad (Rawlings et al., 2012). They are synthesized as inactive precursors that are normally activated in the acidic environment of lysosomes. For this reason, they were considered as, primarily, being involved in non-specific catabolism of intracellular proteins (Turk et al., 2000, Turk et al., 2001). However, cathepsins have been found to regulate a number of other important physiological and pathological processes (reviewed in (Pislar and Kos, 2014)). Many studies have been focused on cathepsins B, L, and S that appear to be most active proteases in the inflammatory response and play a key role in the neurotoxic effects (reviewed in (Pislar and Kos, 2014)). In contrast, cathepsin X has been far less studied in this respect.

The role of cathepsin X, a cysteine cathepsin with solely carboxypeptidase activity, is restricted to cells of the immune system, predominantly monocytes, macrophages, and dendritic cells (Kos et al., 2005, Kos et al., 2009). Cathepsin X expression and proteolytic activity were recently found to be strongly upregulated in mouse brain, in particular in glial cells and aged neurons (Wendt et al., 2007, Hafner et al., 2013). Its association with inflammation-induced neurodegeneration has also been reported (Stichel and Luebbert, 2007). The neurodegenerative action of cathepsin X involves the sequential cleavage of the C-terminal amino acids of γ-enolase that abolishes its neurotrophic activity (Obermajer et al., 2009). In this way, neuronal survival and neuritogenesis, mediated by active γ-enolase inside the cells and that which is released from microglia, can be regulated, leading to impaired neuroprotection (Hafner et al., 2012, Hafner et al., 2013). Additionally, cathepsin X plays an important role in the neuronal injury induced by the neurotoxic stimulant 6-hydroxydopamine (6-OHDA), and could thus be involved in chronic neurodegenerative disorders resulting from progressive loss of dopaminergic neurons in the substantia nigra (Pislar et al., 2014). Substantially increased secretion of cathepsin X from microglia has been observed in response to the inflammatory stimulus induced by lipopolysaccharide (LPS) that induces death of the nigral dopaminergic neurons through microglial activation (Wendt et al., 2009). However, the role of cathepsin X in neuroinflammation and the underlying mechanism remain elusive.

For these reasons, we have examined the expression pattern, release and cell localization of cathepsin X and its proteolytic target, γ-enolase, in LPS-stimulated microglial BV2 and EOC 13.31 cells. Using the cathepsin X specific inhibitor AMS36, cathepsin X inhibition has been shown to play an anti-inflammatory role in LPS-stimulated microglial cells. Furthermore, the detailed molecular mechanisms underlying the anti-inflammatory and neuroprotective effects of cathepsin X inhibition have been analyzed.

2. Material and Methods

2.1. Cell cultures

Mouse microglial BV2 cells were a generous gift from Dr. Alba Minelli (University of Perugia, Perugia, Italy). Mouse microglial EOC 13.31 cells (CRL-2468) and human SH-SY5Y (CRL-2266) cells from the American Type Culture Collection (Manassas, VA, USA). BV2 and SH-SY5Y cells were cultured in Dulbecco's modified Eagle's medium (DMEM) (Sigma, St. Louis, MO, USA) supplemented with 10% fetal bovine serum (FBS) (HyClone, Logan, UT, USA), 2 mM L-glutamine, 50 U/ml penicillin and 50 µg/ml streptomycin (Sigma). The cells were maintained at 37 °C in a humidified atmosphere of 95% air and 5% CO_2, and grown to 80% confluence. EOC 13.31 cells were grown at 37 °C in DMEM (Sigma) supplemented with mouse macrophage colony stimulating factor 1 (R&D Systems, Minneapolis, M) at a concentration of 20 ng/ml, 10% FBS (Hyclone, Logan, UT), 2 mM L-glutamine (Sigma), 50 U/ml penicillin and 50 µg/ml streptomycin (Sigma) and maintained in a humidified atmosphere containing 5% CO_2. Confluent cells were subcultured two or three times per week using 0.25% trypsin.

2.2. Activation of microglial cells

Confluent BV2 and EOC 13.31 cells were stimulated with LPS at 0.1 to 10 µg/ml (L6529, *Escherichia coli 055:B5*, Sigma) in serum-free medium for 24 h or the time indicated. Successful activation was checked routinely by measurement of nitrite in the culture supernatants, using the Griess reagent system as described below.

When required and 1 h prior to LPS stimulation, microglial cells were pretreated with AMS36, a specific, irreversible inhibitor of cathepsin X (1-10 µM), synthesized as reported (Pislar et al., 2014), or with the γ-ENO peptide (25-100 nM) (custom made by Biosynthesis, Lewisville, TX, USA) that corresponds to the C-terminal 30 amino acid sequence of human brain γ-enolase. After stimulation, the microglial cells were harvested and aliquots of the supernatants taken for ELISAs, activity assays, flow cytometric analysis, western blotting and staining by immunofluorescence. In the case of the co-culture model, the supernatants of microglial cells were collected, centrifuged (1200X*g*, 5 min) to remove any cellular material, and transferred to cultured neuroblastoma SH-SY5Y cells.

2.3. The microglial culture supernatant (MCS) transfer model

To test the effect of soluble factors secreted by activated microglia, confluent SH-SY5Y cells were cultured in complete medium and treated, for 24 h, with the supernatants of stimulated microglial BV2 cells containing 1 µg/ml LPS and in the absence or presence (1 or 10 µM) of AMS36. After transfer of the MCS, SH-SY5Y cells were examined for neuronal viability and caspase activity, and by signaling pathway analysis and immunofluorescence staining.

2.4. Quantification of nitrite

After LPS stimulation, as described above, aliquots of the cell supernatants were removed and either stored at -80 ºC or used immediately for determination of nitrite content as an indicator of nitric oxide (NO) production (Liu et al., 2014). Accumulation of NO in culture supernatants was determined by the Griess reagent system (Promega, Madison, WI, USA), in accordance with the manufacturer's instructions. Absorbance was measured with an automatic microplate reader (Tecan Safire^2, Switzerland) at 550 nm. $NaNO_2$ was used as the standard in calculating nitrite concentrations (µM).

2.5. ELISAs

To prepare culture supernatants and cell lysates for analysis of the protein levels of cathepsin X and γ-enolase, BV2 and EOC 13.31 cells were first stimulated as described above. The microglial culture supernatants were then collected, centrifuged and stored at -80 ºC. The cells were washed with phosphate buffered saline (PBS), pH 7.4, harvested in cell lysis buffer (0.05 M sodium acetate buffer, pH 5.5, 1 mM EDTA, 0.1 M NaCl, 0.25% Triton X-100) and stored at -80 ºC. Total protein concentration was determined by DC™ Protein Assay (Bio-Rad, Hercules, CA, USA). Cathepsin X was determined by ELISA, performed as reported (Kos et al., 2005), using goat anti-cathepsin X AF934 antibody (RD Systems, MN, USA) as capture antibody and mouse anti-cathepsin X 3B10 monoclonal antibody conjugated with horseradish peroxidase (HRP) as detection antibody. To measure active γ-enolase, microtiter plates were coated with equal aliquots of the protein in 0.01 M carbonate/bicarbonate buffer, pH 9.6, at 4 ºC. After blocking with 2% bovine serum albumin (BSA) in PBS, pH 7.4, for 1 h at room temperature, mouse antibody against C-terminal γ-enolase (Santa Cruz Biotechnology, CA, USA), suitable for detecting its active form, was added. Following 2 h incubation at 37 ºC, the wells were washed and filled with anti-mouse antibody conjugated with HRP. After further 2 h incubation at 37 ºC, 200 µg/well of TMB substrate in 0.012% H_2O_2 was added. After 15 min, the reaction was stopped by adding 50 µl of 2 µM H_2SO_4. The amount of cleaved substrate was determined by measuring the absorbance at 450 nm, and the protein levels of cathepsin X and γ-enolase were expressed relative to those in untreated cells (control).

2.6. Cathepsin X activity

Cathepsin X activities in cell lysates and culture supernatants of activated microglial cells were measured with the cathepsin X-specific, intramolecularly quenched fluorogenic substrate Abz-Phe-Glu-Lys(Dnp)-OH, synthesized by Jiangsu Vcare Pharmatech Co. (China) as desrcribed previously (Pislar *et al.,* 2014). After stimulation, culture supernatants were collected, centrifuged and stored at -80 ºC until used. Cell lysates were prepared in lysis buffer (0.05 M sodium acetate, pH 5.5, 1 mM EDTA, 0.1 M NaCl, 0.25% Triton X-100) and protein concentration was determined. An aliquot of 100 µl of microglial culture supernatant was incubated at 37 ºC with an aliquot of 100 µg of lysate proteins, followed by measurement of cathepsin X activity using 10 µM Abz-Phe-Glu-Lys(Dnp)-OH. The fluorometric reaction was quantified at 37 ºC at an excitation wavelength of 320 nm and emission wavelength of 420 nm on a microplate reader (Tecan Safire^2). Values are presented as change of fluorescence as a function of time (ΔF/Δt) and cathepsin X activity was expressed relative to that of untreated cells (control).

2.7. Cell viability

Cell viability was evaluated by [3-(4,5-dimethylthiazol-2-yl)-5-(3-carboxymethoxyphenyl)-2-(4-sulfophenyl)-2H-tetrazolium (MTS) assay. BV2 and SH-SY5Y cells were seeded in complete medium in 96-well culture plates in quadruplicate (2 x 10^4/well). The next day, cells were treated as described above and, after the times indicated, cell viability was assessed using the CellTiter 96® Aqueous One Solution Cell Proliferation Assay (Promega), in accordance with the manufacturer's instructions. The absorbance was measured with an automatic microplate reader (Tecan Safire^2) at 490 nm. Values are expressed as a percentage of the untreated cells (control).

2.8. Cytokine assay

Cytokine release from cells was measured in culture supernatants obtained by centrifugation at 1200 rpm for 5 min and stored at -80 ºC until measurement. Cytokine production was assessed by flow cytometry using a BD cytometric bead array - human inflammatory cytokine kit containing beads for determining interleukin-6 (IL-6) and tumor necrosis factor α (TNF-α) (BD Biosciences; San Diego, CA, USA). Flow cytometric analysis was performed using a FACS Calibur flow cytometer with sorting option: four-color and CELLQuest software (BD Biosciences). Standard curves were generated using recombinant cytokines provided in the kit. The data were analyzed with FlowJo software (Tree Star, Inc.; Ashland, OR, U.S.A.).

2.9. Determination of intracellular reactive oxygen species (ROS)

Intracellular ROS generation was determined by staining the cells with dichlorofluorescein diacetate (DCFH-DA) probe (Sigma), using flow cytometry. BV2 cells were seeded in 24-well culture plates in duplicate (2 x 10^5/well) in complete medium. The next day, cells were treated as described above. Following 6 h stimulation, cells were washed with PBS and incubated with 10 μM DCFH-DA in pre-warmed PBS for 20 min at 37 ºC. The cells were then washed again with PBS, resuspended in culture medium, and analyzed by a FACS Calibur flow cytometer (BD Biosciences). The intensity of DCFH-DA fluorescence of the cells served as a measure of ROS production. Data were analyzed using FlowJo software (Tree Star, Inc.) and values are expressed as fold increase of ROS production relative to that of untreated cells (control).

2.10. Caspase 3/7 activity assay

The activity of caspase 3/7 was measured in total cell lysates of BV2 and SH-SY5Y cells (1 x 10^6/mL) stimulated as described above. After 24 h stimulation, cell lysates were prepared and caspase 3/7 activity was measured utilizing a fluorescent Ac-DEVD-AFC peptide substrate (Bachem, Bubendorf, Switzerland) as described (Murn et al., 2004). Fluorescence was monitored continuously for 30 min using a fluorescence microplate reader (Tecan Safire^2) at an excitation wavelength of 405 nm and emission wavelength of 535 nm. Values are presented as change of fluorescence as a function of time and caspase 3/7 activity was expressed relative to that of untreated cells (control).

2.11. Detection of apoptosis

Apoptosis was detected and quantified using an Annexin–FITC Apoptosis Detection Kit (Sigma), in accordance with the manufacturer’s instructions. BV2 cells were cultured in a 24-well plate (2 x 10^5/well) in complete medium. The next day, cells were treated as described above. Following 24 h incubation, cells were washed with cold PBS and re-suspended in 500 µl of binding buffer. FITC-labeled Annexin V (5 µl) and PI (10 µl) were added to the cells and incubated for 15 min in the dark. Cell apoptosis was analyzed using a FACS Calibur flow cytometer (BD Bioscience). The percentage of apoptotic cells (Annexin V-positive cells) was evaluated using FlowJo software and the results presented as percentages of apoptotic cells.

2.12. Flow cytometry analysis of phosphorylated proteins

ERK phosphorylation in SH-SY5Y cells was determined by staining the cells with antibody recognizing ERK2 phosphorylation at Tyr204, using flow cytometry. SH-SY5Y cells were seeded in 24-well culture plates in duplicate (2 x 10^5/well) in complete medium. The next day, cells were treated microglial culture supernatants as indicated above. Following 6 h stimulation, cells were washed with PBS, fixed with 5 % formalin for 10 min at room temperature and further permeabilized with ice-cold methanol for 20 min at 4 ºC. Nonspecific staining was blocked with 3% BSA in PBS for 30 min. Next, cells were incubated with specific antibody to ph-ERK-2 [Tyr204] (Santa Cruz Biotechnology) at the dilution recommended by the manufacturer, in blocking buffer for 45 min at 4 ºC and subsequently incubated with Alexa-Fluor-488-conjugated secondary antibodies for an additional 30 min at room temperature, protected from light. Finally, cells were washed twice with PBS and analyzed by flow cytometry (FACS Calibur, BD Biosciences). Data were analyzed using FlowJo software (Tree Star, Inc.) and values are expressed as fold increase of ERK2 phosphorylation relative to that of untreated cells (control).

2.13. Immunoprecipitation and Western blot analysis

For immunoprecipitation, cells were seeded in 25 cm^2 flasks (5 x 10^6/well), and for detection of signaling kinases in cell lysates, cells were seeded in 6-well plates (2 x 10^6/well). After stimulation at indicated time, cells were harvested in cell lysis buffer (50 mM HPES, pH 6.5, 150 mM NaCl, 1 mM EDTA, 1% Triton X-100) supplemented with a cocktail of protease and phosphatase inhibitors, and incubated for 30 min on ice. Protein determination and western blotting were performed as described (Hafner et al., 2012).

For immunoprecipitation, the protein concentrations were adjusted by adding lysis buffer, pH 8.0, to a final concentration of 100 µg in 50 µl. Then 5 µg of mouse anti-α-enolase-specific antibody, mouse anti-γ-enolase-specific antibody or IgG control antibody (Santa Cruz Biotechnology) were added and incubated overnight at 4 ˚C. To purify the immune complexes, 50 µl of this mixture was added to washed protein A-Sepharose beads (Amersham Pharmacia Biotech AB, Uppsala, Sweden) and mixed for additional 2 h at 4 ˚C. The beads were then washed with binding buffer (0.14 M phosphate buffer), pH 8.2, and the immune complexes eluted by boiling in SDS sample buffer.

For western blot, the following primary antibodies were applied: goat anti-cathepsin X (1/500, R&D Systems), rabbit anti-phospho-p38 (1:1000; Cell Signaling, MA, USA), rabbit anti-phospho-Jun-N-terminal kinase (JNK) (1:50; Santa Cruz Biotechnology), rabbit anti-phospho-ERK1/2 (1:2000; Cell Signaling), rabbit anti-ERK1 (1:1000; Santa Cruz Biotechnology), rabbit anti-p38 (1:1000; Cell Signaling), rabbit anti-JNK (1:1000; Cell Signaling), rabbit anti-ERK2 (1:5000; Santa Cruz Biotechnology) and mouse β-actin (1:500; Sigma). Signals from anti-goat HRP-conjugated (1/5000, Santa Cruz Biotechnology), anti-rabbit or anti-mouse HRP-conjugated secondary antibodies (1:5000; Millipore) were visualized with an enhanced chemiluminescence detection kit (Thermo Scientific, Rockford IL, USA). The band intensities were quantified using Gene Tools software (Sygene, UK), and expressed as values relative to those of controls.

2.14. Immunofluorescence staining

For co-localization of cathepsin X with LAMP1, clathrin or γ-enolase, microglial BV2 cells were cultured on glass coverslips (2 x 10^4/ml) in 24-well culture plates and, next day, stimulated as indicated above for 24 h. The cells were then fixed with 5% formalin at room temperature for 30 min and permeabilized with 0.05% Tween 20 for 10 min. Non-specific staining was blocked with 3% BSA in PBS, pH 7.4 for 30 min. Cells were then incubated with goat anti-cathepsin X (1:500; R&D System), rabbit anti-LAMP1 (1/100; Sigma), mouse anti-clathrin (1:1000; Abcam, Cambridge, UK) or mouse anti-γ-enolase (1:20; Santa Cruz Biotechnology) antibodies in blocking buffer, for 2 h at room temperature. The cells were washed with PBS and further incubated for an additional 2 h with Alexa Fluor 488- and Alexa Fluor 555-labeled secondary antibodies (Molecular Probes, Eugene, OR, USA). After washing with PBS, the Prolong Antifade kit (Molecular Probes) was used for mounting coverslips on glass slides. Fluorescence microscopy was performed using Carl Zeiss LSM 710 confocal microscope (Carl Zeiss, Oberkochen, Germany) with ZEN 2011 image software. The relative co-localization areas were analyzed for several cells (cell number ≥ 10). The quantification of co-localization areas is presented by the average of the pixels in the third quadrant in scatter plot of two fluorescence intensities. The secondary antibody control was also performed in parallel to each experiment (Suppl. Fig. 1A, 1B).

2.15. Statistical analysis

Results shown are representative of at least two independent experiments, each performed in, at least, duplicate, and are presented as means ± SD. ANOVA test and post hoc analysis for multiple comparisons using Dunnett's multiple comparisons *t*-test using GraphPad Prism, version 6 was used for statistical evaluation when two sets of values were compared; $P < 0.05$ was considered to be statistically significant.

3. Results

3.1. LPS-induced regulation of cathepsin X and its substrate γ-enolase in activated microglial cells

Activated microglia release mediators, such as inflammatory molecules or neurotrophic factors, that display either harmful or beneficial effects on neuronal survival and signaling (Li et al., 2007). The amounts of released factors depend on the intensity of stimulation and on time; therefore we first determined whether microglial cells modulate the expression of cathepsin X, by following activation by LPS, in a concentration- or a time-dependent manner. For this purpose, microglial cells BV2 were stimulated for 24 h with 0.1 to 10 µg/ml LPS. Microglial activation was confirmed by an increase in nitrite concentration in the cell culture supernatants (Fig. 1A). Following stimulation, the total level of cathepsin X protein in cell lysates, determined by ELISA, was found to be slightly elevated at higher concentrations of LPS (1 and 10 µg/ml) (Fig. 1B). However, LPS stimulation at 1 µg/ml increased significantly the concentration of cathepsin X in the culture supernatant of BV2 cells (Fig. 1B). Supporting the results of the ELISA, the activity of cathepsin X was similarly increased after LPS stimulation in culture supernatants, the most pronounced effect being at 1 µg/ml of LPS. However, in cell lysates, the activity of cathepsin X was lower (Fig. 1C). When analyzing the time-dependence of LPS stimulation, the effect of LPS (1 µg/ml) stimulation on cathepsin X activity was found to be most evident after 24 h of stimulation (Fig. 1D). These results were confirmed for murine microglial EOC 13.31 cells, in which cathepsin X release and its activity in culture supernatants was again increased in an LPS concentration dependent manner (Suppl. Fig. 2A-C).

Intrigued by the fact that cathepsin X intra- and extracellular protein levels were altered significantly in activated BV2 cells, we further studied the vesicular localization of cathepsin X that followed LPS stimulation for 24 h. In control BV2 cells, a strong localization of cathepsin X in lysosomal structures was observed using lysosomal marker LAMP1; however, it was less prominent in activated microglial cells (Fig. 1E). Additionally, the co-localization of cathepsin X with vesicles containing clathrin was studied. Similarly, LPS stimulation reduced co-localization of cathepsin X with clathrin in microglial cells compared to co-localization in control cells; however the reduction was not significant (Fig. 1F).

In our previous study (Hafner et al., 2013), γ-enolase was shown to be present in mouse microglia EOC 13.31 cells and strongly co-localized with cathepsin X in the perimembrane region. Additionally, the upregulation of γ-enolase in microglial cells in response to neurotoxic stimulus was demonstrated (Hafner et al., 2013). Here, it was further investigated as to whether LPS-activated microglia regulate γ-enolase. The results of the ELISA indicate that LPS stimulation of BV2 cells has no effect on expression of the active form of γ-enolase; detected by using a specific antibody that recognizes the intact C-terminal end of γ-enolase. However, the level of active γ-enolase in the culture supernatants of the BV2 cells was significantly decreased. This coincided with the increasing concentration of the stimulating LPS (0.1 – 10 µg/ml) (Fig. 2A). Similarly, LPS stimulation of EOC 13.31 cells resulted in a significantly reduced level of active γ-enolase in culture supernatants that was most evident at the highest concentration of LPS (2.5 µg/ml), whereas no change in protein level of active γ-enolase was observed in cell lysates (Suppl. Fig. 3A). Nevertheless, the decreased levels of active γ-enolase were reversed in the presence of the specific inhibitor of cathepsin X AMS36 (10 µM), as seen in the culture supernatants of BV2 (Figure 2B) and EOC 13.31 cells (Suppl. Fig. 3B). This indicates that cathepsin X is a regulator of γ-enolase activity in LPS-activated microglia. In order to evaluate the association of cathepsin X with γ-enolase in activated microglia, their co-localization was studied. On following LPS stimulation for 24 h, more extensive co-localization was observed at the plasma membrane in these BV2 cells than on unstimulated BV2 cells (Fig. 2C). In addition, the interaction of cathepsin X with γ-enolase in BV2 cells was identified. We immunoprecipitated putative cathepsin X/γ-enolase complexes from unstimulated and LPS-stimulated BV2 cells. The interaction was observed between cathepsin X and γ-enolase in unstimulated control cells. However, the stimulation of BV2 celles with LPS (1 µg/ml) for 24 h, resulted in an increase of the cathepsin X immunoprecipitated with γ-enolase. No immunoprecipitation was observed when using antibody to α-enolase, and control antibody (mouse IgG), indicating on the specificity of the interaction (Fig. 2D).

3.2. Inhibition of cathepsin X reduces microglial activation

In an attempt to understand the involvement of cathepsin X in microglia activation, BV2 cells were pre-incubated with cathepsin X inhibitor AMS36 (1 and 10 µM) for 1 h, prior to LPS stimulation, and NO production quantitated. In the absence of LPS stimulation, addition of AMS36 did not lead to any change in levels of NO whereas, when followed by LPS stimulation, they increased significantly (Fig. 3A). In comparison to LPS stimulated cells, the level of NO was significantly reduced in the supernatants of activated BV2 cells pretreated with AMS36 at 10 µM (Fig. 3A).

To evaluate the impact of the latter result we studied the release of pro-inflammatory cytokines, IL-6 and TNF-α, in the culture supernatant. BV2 cells were treated with LPS for 24 h in the absence and presence of AMS36 (1 and 10 µM). AMS36 alone did not elicit any marked alteration in release of cytokines, whereas LPS stimulation significantly increased the levels of both cytokines (Fig. 3B and C). Pretreatment with AMS36 at 10 µM prior to LPS stimulation significantly reduced IL-6 and TNF-α production (Fig. 3B and C), indicating that inhibition of cathepsin X reduced microglial activation.

3.3. Cathepsin X inhibition reduces apoptosis and activation of MAP kinases in activated microglia

LPS induces microglial cell death by apoptosis (Lee et al., 2001b). Treatment of BV2 cells with LPS (1 µg/ml) for 24 h and 48 h decreased their viability, found to be significant at 48 h (Fig. 4A). Pre-incubation of BV2 cells with AMS36 (1-10 µM) for 1 h partially reversed the effect of LPS stimulation at 48 h, but only at a higher a concentration of inhibitor (10 µM of AMS36) (Fig. 4B). The effect of γ-ENO peptide, which mimics the C-terminal end of active γ-enolase, the latter being shown to be increased in the supernatant of activated microglia, was also studied. At a higher concentration (100 nM), it enhanced the viability of unstimulated BV2 cells and, moreover, the peptide was observed to protect against LPS toxicity (Fig. 4C). These results suggest that inhibition of cathepsin X, which preserves γ-enolase in its active form, significantly reduces LPS-mediated microglial cell death.

ROS are additional factors that can induce several signaling pathways, leading to microglial death during inflammation in response to extracellular stimuli such as bacterial LPS (Dilshara et al., 2014). We therefore studied the effect of cathepsin X inhibitor AMS36 on ROS production in LPS-stimulated BV2 microglial cells. Cytometric analysis showed that AMS36 significantly reduced LPS-induced ROS production after 6 h stimulation at both 1 and 10 µM (Fig. 5A). In addition, caspase 3 activity was measured in cell lysates of LPS stimulated BV2 cells. Inflammatory stimuli trigger activation of the caspase cascade, ultimately leading to apoptosis (Lee et al., 2001a). Caspase 3, an executor of caspase cascade, was activated in BV2 cells in response to an LPS stimulus, whereas AMS36 significantly decreased this activation in a concentration-dependent manner (Fig. 5B). The effect of cathepsin X inhibitor on LPS-induced microglial apoptosis was confirmed by an Annexin V/PI staining assay using flow cytometry (Fig. 5C), in which the reduction of microglial apoptosis correlated well with the reduced viability of microglial cells in the presence of AMS36 after LPS stimulation.

MAPKs play important roles in modulating the expression of the pro-inflammatory response in LPS-stimulated microglia (Kim et al., 2004, Jack et al., 2005). Pretreatment of BV2 cells with AMS36 markedly blocked LPS-induced p38 and JNK activation (Fig. 6A and B), and also reduced LPS-induced phosphorylation of ERK1 and ERK2 (Fig. 6C). These results suggest that cathepsin X is indeed involved in inflammatory signaling in LPS-stimulated microglia.

3.4. Inhibition of cathepsin X abrogates microglia-mediated neurotoxicity

Microglia, when activated, could induce neuronal cell degeneration by releasing inflammatory mediators and cytokines (Kaushal and Schlichter, 2008, Saijo et al., 2009). We therefore investigated whether increased levels of cathepsin X in the MCS could contribute to the relief of activated microglia–induced neurotoxicity. For this purpose, microglial cells were activated with LPS in the absence and in the presence of cathepsin X inhibitor AMS36 at 1 µM and 10 µM for 24 h, and the resulting MCS added to cultures of neuronal SH-SY5Y cells. The viability of neuronal cells was assessed 48 h later by MTS assay. The viability of SH-SY5Y cells treated with MCS from unstimulated BV2 cells did not differ significantly from that for control cells treated with the complete medium for SH-SY5Y cells, whereas treatment with MCS from LPS-activated BV2 cells (MCS[LPS]) resulted in a significant reduction of neuronal viability 48 h after transfer. However, the neurotoxic effect of MCS collected from activated BV2 cells pretreated with AMS36 (MCM[AMS36/LPS]) was reduced in a concentration dependent manner (Fig. 7A). Cell death induced by culture supernatant of activated microglia was further confirmed by analyzing the activity of caspase-3, an executor of apoptotic cell death. SH-SY5Y cells treated with MCS[LPS] for 24 h showed increased caspase-3 activity in contrast to those treated with complete medium or MCS of unstimulated microglia, whereas treatment with AMS36 prior to LPS stimulation of BV2 cells (MCS[AMS36/LPS]) led to a smaller increase of caspase-3 activity in neuronal cells (Fig. 7B). These results suggest that cathepsin X released from activated microglia contributes to the neuroinflammatory response that is reflected in neuronal death and in inhibited neurite outgrowth.

5. Discussion

Microglia play an important role in inflammatory responses in the CNS. Activated microglia secrete large amounts of neurotoxic factors, such as NO, TNF-α and IL-6, that promote neurodegeneration and contribute to neuronal loss (Gonzalez-Scarano and Baltuch, 1999, Nakanishi, 2003a). In addition to inflammatory cytokines, activated microglia also secrete cathepsins, including cathepsin X (Wendt et al., 2009). This study has revealed the role of cathepsin X in LPS-induced neuroinflammation. LPS is shown to regulate the levels of cathepsin X and its substrate γ-enolase in microglial BV2 and EOC 13.31 cells. Further, inhibition of cathepsin X with AMS36 blocks the release of the active form of γ-enolase from LPS stimulated microglia cells, attenuating NO production and secretion of pro-inflammatory cytokines IL-6 and TNF-α. The underlying molecular mechanism of the inhibitory effect is indicated by the facts that AMS36 was shown to reduce the probability of LPS-induced microglia cell death by suppressing intracellular ROS production and caspase-3 activity and by regulating the MAPK signaling pathway. Moreover, inhibition of microglial cathepsin X was shown to be neuroprotective against microglia-derived factors in neuronal cells.

Alterations in the expression patterns and localization of the lysosomal cathepsins in the central nervous system have been reported in normal, aged brain and under pathological conditions (Nakanishi, 2003b, Wendt et al., 2007, Hafner et al., 2013). Cathepsin X expression and proteolytic activity were found to be strongly upregulated in the mouse brain, in particular in glial cells and aged neurons (Wendt et al., 2007, Hafner et al., 2013), and their association with inflammation-induced neurodegeneration has also been reported (Stichel and Luebbert, 2007). In response to LPS, an inflammation elicitor that induces death of the nigral dopaminergic neurons through microglial activation, a substantial increase in cathepsin X secretion from microglial cells has been observed (Hunter et al., 2009, Wendt et al., 2009). In addition, levels of cathepsin X protein were significantly increased in the cytoplasm of activated microglial cells (Wendt et al., 2009). In our study, increased levels of cathepsin X were demonstrated in the culture supernatants in response to LPS stimulation, using two microglial cell lines, BV2 and EOC 13.31. The increase of secretion was dependent on the level of the stimulus, 1 µg/ml being the most effective concentration. Likewise, the proteolytic activity of cathepsin X in the culture supernatant of activated microglial cells was increased by prior LPS stimulation. It is postulated that the functions of microglia, either neuroprotective or neurotoxic, are determined by the equilibrium between various factors that depend on the concentration of the stimulant, e.g. LPS (Li et al., 2007). Higher concentrations of LPS (≥ 1 µg/ml) promote neurotoxic microglial function through release of pro-inflammatory mediators and cytokines (Li et al., 2007). Similarly, secreted cathepsin B has been shown to be a major causative factor of microglia-induced neuronal apoptosis (Kingham and Pocock, 2001). During LPS-induced inflammation, cathepsin B is also translocated from lysosomes to other subcellular compartments in hippocampal neurons (Czapski et al., 2010). Higher concentrations of LPS significantly induce the release and activity of cathepsin X, a protease shown to play an active role in apoptosis of dopaminergic neurons (Pislar et al., 2014). As for cathepsin B, altered localization of cathepsin X was observed in activated microglial cells. The less prominent lysosomal and clathrin vesicular localization of cathepsin X, following LPS stimulation and noted in BV cells, is in line with the increased release of cathepsin X from microglial cells in response to LPS stimulus.

Microglial cells are also a source of growth factors, suggesting that they provide trophic support for glia and neurons (Elkabes et al., 1996). Activated microglia have been linked with neuroprotection in several studies, and it has been suggested that glial cells are activated in response to neuronal injury, with subsequent release of neurotrophic factors, such as nerve growth factor, brain-derived neurotrophic factor, neurotrophin-3 and neurotrophin-4/5, that exhibit neuroprotective effects (Mallat et al., 1989, Lindsay et al., 1994, Elkabes et al., 1996, Nakajima et al., 2001). Neurotrophic activity has been reported for the C-terminal end of γ-enolase (Hattori et al., 1995, Hafner et al., 2012) that is needed for its translocation towards the plasma membrane. When cleaved by cathepsin X, the translocation and neurotrophic activity of γ-enolase are attenuated (Hafner et al., 2010). γ-

Enolase has been used for many years as a marker of neuronal loss (Herrmann and Ehrenreich, 2003) and is expected to be present in brain tissue in neuronal cells. However, it was recently shown to be present also in the microglial cells surrounding the senile plaques in Tg2576 transgenic mice, where it has a neuroprotective role in amyloid-β-related neurodegeneration (Hafner et al., 2013, Pislar and Kos, 2013). Here we showed that increased concentrations of LPS result in significantly reduced release of active γ-enolase from activated BV2 and EOC 13.31 cells. This observation coincides with that of the increased activity, at higher concentrations of LPS, of cathepsin X which is capable of cleavage and inactivation of γ-enolase. The interaction of cathepsin X with γ-enolase in microglial BV2 cells was confirmed by the immunoprecipitation study, where LPS stimulation strongly increased their association in cells. This result are in line with the study of the co-localization of cathepsin X and γ-enolase, which demonstrates stronger association of these two proteins at the plasma membrane in BV2 cells following LPS stimulation. This suggests that the lower levels of active γ-enolase in the culture supernatant of activated microglial cells are the result of cathepsin X cleavage. Nevertheless, pretreatment of microglial cells with a specific inhibitor of cathepsin X not only reversed the decrease of the level of active γ-enolase in the culture supernatant of LPS-activated microglia, but also enriched the microglial supernatant with the active form of γ-enolase that is able to exert neurotrophic and neuroprotective effects.

Activated microglia release a variety of neurotoxic mediators, including cathepsin X. Inhibition of activated microglia could thus serve as a key mechanism for the treatment of inflammation-associated neurological disorders. We demonstrated that the specific irreversible inhibitor of cathepsin X, AMS36, reduces excessive release of NO, a marker of activated microglia, whereas the basal NO level is not reduced after treatment with the inhibitor. Furthermore, inhibition of cathepsin X with AMS36 reduced the LPS-induced elevated levels of IL-6 and TNF-α in culture supernatants of BV2 cells. Although IL-6 may promote the survival, differentiation and growth of neurons, it has been shown to reduce hippocampal neurogenesis (Vallieres et al., 2002) and is therefore considered to be the pro-inflammatory mediator (Frei et al., 1989) similar as known for TNF-α (Sawada et al., 1989). The TNF-α released from activated microglia mediates neurotoxicity and can cause neuronal cell death, either directly or indirectly via the induction of the formation of NO and free radicals in glial cells (Zajicek et al., 1992, Hu et al., 1997). Thus, suppression of NO, IL-6 and TNF-α formation by the inhibition of cathepsin X contributes to reduced neurotoxic effects of activated microglia.

Microglial cells undergo apoptosis on inflammatory activation in a manner similar to that of the activation-induced cell death of lymphocytes, in which process NO is a major autocrine mediator (Lee et al., 2001b, Suk et al., 2001). Inflammatory stimuli such as LPS play multiple roles in microglial apoptosis. LPS not only induces cytotoxic NO production, but also initiates the NO-independent apoptotic pathway by inducing the caspase cascade (Lee et al., 2001a). Here, the viability of BV2 cells was observed to be reduced following LPS stimulation, in line with other studies (Lee et al., 2001a, Jung et al., 2005, Kacimi et al., 2011). Furthermore, inhibition of cathepsin X not only suppressed microglial activation, and consequently the inflammatory response through reduced NO and ROS production, but also affected the viability of microglial cells on LPS stimulation. Thus inhibitor AMS36 diminished the degree of LPS-induced reduction of BV2 cell viability. An identical effect was observed in the presence of the peptide mimicking the active C-terminal end of γ-enolase, additionally highlighting the link between cathepsin X proteolytic activity and the degree of microglial apoptosis. We further demonstrated that inhibition of cathepsin X suppresses LPS induced apoptosis. When cells were exposed to LPSs, they underwent early apoptosis and late apoptosis/death and the effect in cell death was more evident as seen in viability assay. However, in the presence of inhibitor AMS36, both apoptotic populations were significantly decreased. The NO-independent cytotoxic mechanism involves upregulated caspase-11 that is autoactivated in microglia and triggers an activation cascade of downstream caspases, ultimately leading to cell apoptosis (Lee et al., 2001a). Caspase-3 is the final executor of caspase-dependent apoptotic damage; its activity was significantly increased in microglial cells upon LPS stimulation. Nevertheless, the activation of caspase-3 in activated BV2 cells was suppressed in the presence of AMS36, suggesting that inhibition of cathepsin X contributes to the inhibition of microglia activation.

The inflammatory response elicited by activated microglia is associated with the activation of MAPKs, and this can lead to a variety of physiological processes such as cell growth, differentiation and apoptotic cell death (Svensson et al., 2011). The MAPK family, that includes JNK, p38 and ERK, plays a critical role in the production of cytokines and mediators associated with the pathogenesis of inflammation (Kacimi et al., 2011). Indeed, LPS induces p38, JNK and ERK activation in BV2 cells, as is well documented (Lee and Kim, 2014, Liu et al., 2014). Pretreatment with cathepsin X inhibitor AMS36 apparently reduced the activation of LPS-induced MAPK kinases, demonstrating that cathepsin X inhibitor-mediated suppressed microglia activation can interfere with MAPK signaling pathways.

In vivo, during neurodegeneration, the toxic factors released from activated microglia cause neuronal death (Glass et al., 2010). Here, we showed that microglial cathepsin X is implicated in degeneration of neuronal cell, where an inhibitor of cathepsin X AMS36 protected cell against LPS toxic effect. The neuroprotective mechanism of the action of AMS36 may include reduced caspase-dependent apoptosis. Pretreatment of BV2 cells with AMS36 upon LPS stimulation significantly decreased caspase-3 activity in SH-SY5Y cells. Activation of the caspase cascade, and consequent induction of apoptosis, has been observed in neuronal cells in response to toxic stimuli such as 6-OHDA (Blum et al., 2001). Our previous study showed the involvement of cathepsin X in 6-OHDA-induced apoptosis in both PC12 and SH-SY5Y cells, and provided evidence that inhibition of cathepsin X protects neuronal cells against neurotoxicity (Pislar et al., 2014). Therefore, these results are in line with protective action on neuronal cells of cathepsin X inhibition.

In conclusion, this study provides a new insight into the involvement of cathepsin X in inflammation-induced neurodegeneration. There is a significant release of cathepsin X from activated BV2 and EOC 13.31 cells following a LPS stimulus that coincides with reduced release of the active form of γ-enolase. Additionally, we demonstrated a protective role for cathepsin X inhibitor AMS36 in LPS-induced neuroinflammation and analyzed the underlying molecular mechanisms, as summarized in Fig. 8. Cathepsin X inhibitor AMS36 suppresses NO and ROS production and attenuates cytokine release from activated microglia, through the inhibition of MAPK signaling pathways. We have also shown that inhibition of cathepsin X activity could be important for preventing and treating neurodegenerative diseases that are associated with excessive microglial activation and subsequent neurotoxic inflammation.

Competing interests

The authors declare the absence of competing interest.

Authors' contributions

AP designed the study, performed the experiments, generated the data for Figures 1-7, prepared Figure 8 and the draft manuscript. BB participated in carrying out the experiments. NZ designed and synthesised the cathepsin X inhibitor AMS36. JK coordinated the research, reviewed the manuscript and supervised the study. All authors read and approved the final manuscript.

Acknowledgements

We acknowledge Professor Roger Pain for critical review of the paper before submission. We also thank Dr. Martina Gobec for CBA human inflammatory cytokine kit. This study was supported by the Research Agency of Republic of Slovenia (P4-0127 JK).

References

Blum D, Torch S, Lambeng N, Nissou M, Benabid AL, Sadoul R, Verna JM. 2001. Molecular pathways involved in the neurotoxicity of 6-OHDA, dopamine and MPTP: contribution to the apoptotic theory in Parkinson's disease. Prog Neurobiol. 65,135-172.

Clark AK, Malcangio M. 2012. Microglial signalling mechanisms: Cathepsin S and Fractalkine. Exp Neurol. 234, 283-292.

Czapski GA, Gajkowska B, Strosznajder JB. 2010. Systemic administration of lipopolysaccharide induces molecular and morphological alterations in the hippocampus. Brain Res. 1356, 85-94.

Dilshara MG, Lee KT, Choi YH, Moon DO, Lee HJ, Yun SG, Kim GY. 2014. Potential chemoprevention of LPS-stimulated nitric oxide and prostaglandin E(2) production by alpha-L-rhamnopyranosyl-(1-->6)-beta-D-glucopyranosyl-3-indolecarbonate in BV2 microglial cells through suppression of the ROS/PI3K/Akt/NF-kappaB pathway. Neurochem Int. 67, 39-45.

Elkabes S, DiCicco-Bloom EM, Black IB. 1996. Brain microglia/macrophages express neurotrophins that selectively regulate microglial proliferation and function. J Neurosci. 16, 2508-2521.

Fan K, Li D, Zhang Y, Han C, Liang J, Hou C, Xiao H, Ikenaka K, Ma J. 2015. The induction of neuronal death by up-regulated microglial cathepsin H in LPS-induced neuroinflammation. J Neuroinflammation. 12, 54.

Fan K, Wu X, Fan B, Li N, Lin Y, Yao Y, Ma J. 2012. Up-regulation of microglial cathepsin C expression and activity in lipopolysaccharide-induced neuroinflammation. J Neuroinflammation. 9, 96.

Frei K, Malipiero UV, Leist TP, Zinkernagel RM, Schwab ME, Fontana A. 1989. On the cellular source and function of interleukin 6 produced in the central nervous system in viral diseases. Eur J Immunol.19, 689-694.

Glass CK, Saijo K, Winner B, Marchetto MC, Gage FH. 2010. Mechanisms underlying inflammation in neurodegeneration. Cell 140, 918-934.

Gonzalez-Scarano F, Baltuch G. 1999. Microglia as mediators of inflammatory and degenerative diseases. Annu Rev Neurosci. 22, 219-240.

Hafner A, Glavan G, Obermajer N, Zivin M, Schliebs R, Kos J. 2013. Neuroprotective role of gamma-enolase in microglia in a mouse model of Alzheimer's disease is regulated by cathepsin X. Aging Cell 12, 604-614.

Hafner A, Obermajer N, Kos J. 2010. gamma-1-syntrophin mediates trafficking of gamma-enolase towards the plasma membrane and enhances its neurotrophic activity. Neurosignals 18, 246-258.

Hafner A, Obermajer N, Kos J. 2012. gamma-Enolase C-terminal peptide promotes cell survival and neurite outgrowth by activation of the PI3K/Akt and MAPK/ERK signalling pathways. Biochem J. 443, 439-450.

Hattori T, Takei N, Mizuno Y, Kato K, Kohsaka S. 1995. Neurotrophic and neuroprotective effects of neuron-specific enolase on cultured neurons from embryonic rat brain. Neurosci Res. 21, 191-198.

Herrmann M, Ehrenreich H. 2003. Brain derived proteins as markers of acute stroke: their relation to pathophysiology, outcome prediction and neuroprotective drug monitoring. Restor Neurol Neurosci. 21, 177-190.

Hu S, Peterson PK, Chao CC. 1997. Cytokine-mediated neuronal apoptosis. Neurochem Int. 30, 427-431.

Hunter RL, Cheng B, Choi DY, Liu M, Liu S, Cass WA, Bing G. 2009. Intrastriatal lipopolysaccharide injection induces parkinsonism in C57/B6 mice. J Neurosci Res. 87, 1913-1921.

Jack CS, Arbour N, Manusow J, Montgrain V, Blain M, McCrea E, Shapiro A, Antel JP. 2005. TLR signaling tailors innate immune responses in human microglia and astrocytes. J Immunol. 175, 4320-4330.

Jung DY, Lee H, Jung BY, Ock J, Lee MS, Lee WH, Suk K. 2005. TLR4, but not TLR2, signals autoregulatory apoptosis of cultured microglia: a critical role of IFN-beta as a decision maker. J Immunol. 174, 6467-6476.

Kacimi R, Giffard RG, Yenari MA. 2011. Endotoxin-activated microglia injure brain derived endothelial cells via NF-kappaB, JAK-STAT and JNK stress kinase pathways. J Inflamm. (Lond) 8, 7.

Kaushal V, Schlichter LC. 2008. Mechanisms of microglia-mediated neurotoxicity in a new model of the stroke penumbra. J Neurosci. 28, 2221-2230.

Kettenmann H, Hanisch UK, Noda M, Verkhratsky A. 2011. Physiology of microglia. Physiol Rev. 91, 461-553.

Kim SH, Smith CJ, Van Eldik LJ. 2004. Importance of MAPK pathways for microglial pro-inflammatory cytokine IL-1 beta production. Neurobiol Aging. 25, 431-439.

Kingham PJ, Pocock JM. 2001. Microglial secreted cathepsin B induces neuronal apoptosis. J Neurochem. 76, 1475-1484.

Kos J, Jevnikar Z, Obermajer N. 2009. The role of cathepsin X in cell signaling. Cell Adh Migr. 3, 164-166.

Kos J, Sekirnik A, Premzl A, Zavasnik Bergant V, Langerholc T, Turk B, Werle B, Golouh R, Repnik U, Jeras M, Turk V. 2005. Carboxypeptidases cathepsins X and B display distinct protein profile in human cells and tissues. Exp Cell Res. 306, 103-113.

Lee EJ, Kim HS. 2014. The anti-inflammatory role of tissue inhibitor of metalloproteinase-2 in lipopolysaccharide-stimulated microglia. J Neuroinflammation. 11, 116.

Lee J, Hur J, Lee P, Kim JY, Cho N, Kim SY, Kim H, Lee MS, Suk K. 2001a. Dual role of inflammatory stimuli in activation-induced cell death of mouse microglial cells. Initiation of two separate apoptotic pathways via induction of interferon regulatory factor-1 and caspase-11. J Biol Chem. 276, 32956-32965.

Lee P, Lee J, Kim S, Lee MS, Yagita H, Kim SY, Kim H, Suk K. 2001b. NO as an autocrine mediator in the apoptosis of activated microglial cells: correlation between activation and apoptosis of microglial cells. Brain Res. 892, 380-385.

Li L, Lu J, Tay SS, Moochhala SM, He BP. 2007. The function of microglia, either neuroprotection or neurotoxicity, is determined by the equilibrium among factors released from activated microglia in vitro. Brain Res. 1159, 8-17.

Lindsay RM, Wiegand SJ, Altar CA, DiStefano PS. 1994. Neurotrophic factors: from molecule to man. Trends Neurosci, 17, 182-190.

Liu RP, Zou M, Wang JY, Zhu JJ, Lai JM, Zhou LL, Chen SF, Zhang X, Zhu JH. 2014. Paroxetine ameliorates lipopolysaccharide-induced microglia activation via differential regulation of MAPK signaling. J Neuroinflammation. 11, 47.

Lively S, Schlichter LC. 2013. The microglial activation state regulates migration and roles of matrix-dissolving enzymes for invasion. J Neuroinflammation. 10, 75.

Mallat M, Houlgatte R, Brachet P, Prochiantz A. 1989. Lipopolysaccharide-stimulated rat brain macrophages release NGF in vitro. Dev Biol. 133, 309-311.

Murn J, Urleb U, Mlinaric-Rascan I. 2004. Internucleosomal DNA cleavage in apoptotic WEHI 231 cells is mediated by a chymotrypsin-like protease. Genes Cells 9, 1103-1111.

Nakajima K, Honda S, Tohyama Y, Imai Y, Kohsaka S, Kurihara T. 2001. Neurotrophin secretion from cultured microglia. J Neurosci Res. 65, 322-331.

Nakanishi H. 2003a. Microglial functions and proteases. Mol Neurobiol. 27, 163-176.

Nakanishi H. 2003b. Neuronal and microglial cathepsins in aging and age-related diseases. Ageing Res Rev. 2, 367-381.

Obermajer N, Doljak B, Jamnik P, Fonovic UP, Kos J. 2009. Cathepsin X cleaves the C-terminal dipeptide of alpha- and gamma-enolase and impairs survival and neuritogenesis of neuronal cells. Int J Biochem Cell Biol. 41, 1685-1696.

Pislar A, Kos J. 2014. Cysteine cathepsins in neurological disorders. Mol Neurobiol. 49, 1017-1030.

Pislar AH, Kos J. 2013. C-terminal peptide of gamma-enolase impairs amyloid-beta-induced apoptosis through p75(NTR) signaling. Neuromolecular Med. 15, 623-635.

Pislar AH, Zidar N, Kikelj D, Kos J. 2014. Cathepsin X promotes 6-hydroxydopamine-induced apoptosis of PC12 and SH-SY5Y cells. Neuropharmacology 82, 121-131.

Rawlings ND, Barrett AJ, Bateman A. 2012. MEROPS: the database of proteolytic enzymes, their substrates and inhibitors. Nucleic Acids Res. 40, D343-350.

Saijo K, Winner B, Carson CT, Collier JG, Boyer L, Rosenfeld MG, Gage FH, Glass CK. 2009. A Nurr1/CoREST pathway in microglia and astrocytes protects dopaminergic neurons from inflammation-induced death. Cell 137, 47-59.

Sawada M, Kondo N, Suzumura A, Marunouchi T. 1989. Production of tumor necrosis factor-alpha by microglia and astrocytes in culture. Brain Res. 491, 394-397.

Schindowski K, Belarbi K, Buee L. 2008. Neurotrophic factors in Alzheimer's disease: role of axonal transport. Genes Brain Behav. 7 Suppl 1, 43-56.

Stichel CC, Luebbert H. 2007. Inflammatory processes in the aging mouse brain: participation of dendritic cells and T-cells. Neurobiol Aging. 28, 1507-1521.

Suk K, Lee J, Hur J, Kim YS, Lee M, Cha S, Yeou Kim S, Kim H. 2001. Activation-induced cell death of rat astrocytes. Brain Res. 900, 342-347.

Svensson C, Part K, Kunnis-Beres K, Kaldmae M, Fernaeus SZ, Land T. 2011. Pro-survival effects of JNK and p38 MAPK pathways in LPS-induced activation of BV-2 cells. Biochem Biophys Res Commun. 406, 488-492.

Turk B, Turk D, Turk V. 2000. Lysosomal cysteine proteases: more than scavengers. Biochim Biophys Acta. 1477, 98-111.

Turk V, Turk B, Turk D. 2001. Lysosomal cysteine proteases: facts and opportunities. EMBO J. 20, 4629-4633.

Vallieres L, Campbell IL, Gage FH, Sawchenko PE. 2002. Reduced hippocampal neurogenesis in adult transgenic mice with chronic astrocytic production of interleukin-6. J Neurosci. 22, 486-492.

Wendt W, Schulten R, Stichel CC, Lubbert H. 2009. Intra- versus extracellular effects of microglia-derived cysteine proteases in a conditioned medium transfer model. J Neurochem. 110, 1931-1941.

Wendt W, Zhu XR, Lubbert H, Stichel CC. 2007. Differential expression of cathepsin X in aging and pathological central nervous system of mice. Exp Neurol. 204, 525-540.

Zajicek JP, Wing M, Scolding NJ, Compston DA. 1992. Interactions between oligodendrocytes and microglia. A major role for complement and tumour necrosis factor in oligodendrocyte adherence and killing. Brain 115 (Pt 6), 1611-1631.

Figure legends

Fig. 1. Effects of LPS stimulation on cathepsin X expression and localization in BV2 cells. BV2 cells were stimulated with concentrations of LPS of 0.1 to 10 µg/ml) for 24 h or the time period indicated. **(A)** Nitrite concentration in the culture supernatants of LPS stimulated BV2 cells. Values are means ± SD of five independent experiments. $*P < 0.05$ **(B)** The levels of cathepsin X in cell lysates and culture supernatants of BV2 cells stimulated for 24 h with concentrations of LPS ranging from 0.1 to 10 µg/ml were measured by ELISA, using goat anti-cathepsin X AF934 and mouse anti-cathepsin X 3B10 as capture and detection antibodies, respectively. Values are means ± SD of three independent experiments. $*P < 0.05$ **(C and D)** Cathepsin X activity in cell lysates and culture supernatants determined at concentrations of LPS ranging from 0.1 to 10 µg/ml **(C)** and with 1 µg/ml LPS at the times indicated after stimulation with 1 µg/ml LPS **(D)**, using the cathepsin X-specific substrate Abz-Phe-Glu-Lys(Dnp)-OH. Values are means ± SD of five independent experiments. $*P < 0.05$ **(E)** Representative images of double immunofluorescence staining for LAMP1 (green fluorescence) with cathepsin X (red fluorescence) in unstimulated BV2 cells (Control) and in cells stimulated with 1 µg/ml LPS (LPS) for 24 h. The graph (*right panel*) represents the quantification of the relative co-localization area of LAMP1 and cathepsin X as mean ± SD of the pixels in third quadrant of scatter plot (cell numbers ≥ 10). $*P < 0.05$ *Scale bars* 20 µm **(F)** Representative images of double immunofluorescence staining for clathrin (green fluorescence) and for cathepsin X (red fluorescence) in unstimulated BV2 cells (control) and in cells previously stimulated with 1 µg/ml LPS (LPS) for 24 h. The graph (*right panel*) presents the quantification of relative co-localization area of clathrin and cathepsin X as mean ± SD of the pixels in third quadrant of scatter plot (cell numbers ≥ 10). *Scale bars* 20 µm

Fig. 2. Expression and localization of γ-enolase in LPS-stimulated BV2 cells. Cells were stimulated for 24 h with increasing concentrations of LPS (0.1 -10 µg/ml) either in the absence or

the presence of cathepsin X inhibitor AMS36 (10 µM). **(A)** Levels of active γ-enolase in cell lysates and culture supernatants of BV2 cells stimulated with LPS for 24 h were measured by ELISA, using for capture mouse antibody against C-terminal γ-enolase, suitable for detecting its active form. Values are means ± SD of three independent experiments. **P* < 0.05 **(B)** The levels of active γ-enolase in culture supernatants of BV2 cells pretreated with AMS36 for 1 h prior to LPS stimulation for 24 h, measured by ELISA. Values are means ± SD for three independent experiments. **P* < 0.05 **(C)** Representative images of double immunofluorescence staining for cathepsin X (green fluorescence) and γ-enolase (red fluorescence) in unstimulated BV2 cells (control) and cells stimulated with 1 µg/ml LPS (LPS) for 24 h. The graph (*right panel*) presents the quantification of relative co-localization areas of cathepsin X and γ-enolase as mean ± SD of the pixels in third quadrant of scatter plot (cell numbers ≥ 10). **P* < 0.05 *Scale bars* 20 µm **(D)** Representative images of Western blot after immunoprecipitation. BV2 cells were stimulated with LPS (1 µg/ml) for 24 h. Cells were then lysed and incubated with either mouse α-enolase- or mouse γ-enolase-specific antibody or nonspecific mouse IgG. The immunoprecipitates were analyzed by western blotting probed with goat anti-cathepsin X antibody. Graph showing the relative amount of cathepsin X in the immunoprecipitates after LPS stimulation compared to untreated control BV2 cells.

Fig. 3. Effect of cathepsin X inhibition on LPS-induced release of pro-inflammatory cytokines from BV2 cells. Cells were pretreated with cathepsin X inhibitor AMS36 (1 and 10 µM) for 1 h and then stimulated with LPS at 1 µg/ml for 24 h. **(A)** Nitrite concentration in the culture supernatants of LPS stimulated BV2 cells. Values are means ± SD of five independent experiments. **P* < 0.05 (**B and C**) Release of cytokines, IL-6 **(B)** and TNF-α **(C)** into the culture supernatants of LPS stimulated BV2 cells determined by flow cytometry. Values are means ± SD of two independent experiments. **P* < 0.05

Fig. 4. Effects of cathepsin X inhibitor and active γ-enolase peptide on LPS-induced microglial cell death. (A) BV2 cells were stimulated with LPS at 1 µg/ml for 24 h and 48 h. Cell viability was evaluated by MTS assay. **(B and C)** BV2 cells were pretreated with cathepsin X inhibitor AMS36 (1 and 10 µM) **(B)** or with active γ-enolase peptide γ-ENO (25 and 100 nM) **(C)** for 1 h, then stimulated with LPS (1 µg/ml). After 48 h, cell viability was evaluated by MTS assay. Values are means ± SD of three independent experiments, each performed in quadruplicate. $^*P < 0.05$

Fig. 5. Cathepsin X inhibitor reduces LPS-induced apoptosis in BV2 cells. Cells were pretreated with cathepsin X inhibitor AMS36 (1 and 10 µM) for 1 h, then stimulated with LPS at 1 µg/ml. **(A)** Intracellular ROS levels after 6 h were measured by flow cytometry using a fluorescent DCFH-DA probe. Each value is expressed as the relative percentage of DCF-positive cells normalized to the appropriate control. Values are means ± SD of four independent experiments, each performed in duplicate. $^*P < 0.05$ **(B)** Caspase-3/7 activity in cell lysates following 24 h of stimulation determined fluorometrically using the specific substrate for caspase 3/7 Ac-DEVD-AFC. Each value is expressed as the rate of change of fluorescence ($\Delta F/\Delta t$). Values are means ± SD of four independent experiments, each performed in duplicate. $^*P < 0.05$ **(C)** The percentages of apoptotic cells determined by flow cytometry, using Annexin V and PI staining 24 h, after incubation with LPS in the absence or presence of the inhibitor. The quadrant threshold was set according to control BV2 cells. Cells treated with LPS and apoptotic cells (Annexin V positive cells) were determined. The graph (*right panel*) shows the results of quantitative analysis and indicates the percentage of fraction of cells showing apoptosis (Annexin V positive cells). Results are means ± SD of two independent assays. $^*P < 0.05$

Fig. 6. Effect of cathepsin X inhibitor on LPS-stimulated activation of MAPKs. Cells were pretreated with cathepsin X inhibitor AMS36 (1 and 10 µM) for 1 h and then stimulated with LPS at 1 µg/ml for additional 1 h. Representative images of Western blots for the activation of p38

(**A**), JNK (**B**) and ERK1/2 (**C**), are given. Levels of phosphorylated form of p38, JNK, ERK1 and ERK2 were quantified and normalized to the respective total protein level. Each value is expressed relative to control cells. Values are means ± SD of two independent experiments. *$P < 0.05$

Fig. 7. Neuroprotective effect of cathepsin X inhibitor in a microglial culture supernatant (MCS) transfer model. Microglial BV2 cells were pretreated with cathepsin X inhibitor AMS36 (1 and 10 µM) for 1 h, then stimulated with LPS at 1 µg/ml for 24 h. The microglial culture supernatants (MCS) were transferred to neuronal SH-SY5Y cells. **(A)** Neuronal cell viability evaluated 48 h after MCS transfer from BV2 cells to SH-SY5Y cells by MTS assay. Each value is expressed relative to cells treated with complete SH-SY5Y medium (Control). Values are means ± SD of four independent experiments, each performed in quadruplicate. *$P < 0.05$ **(B)** Caspase-3/7 activity in cell lysates of SH-SY5Y cells measured 24 h after MCS transfer using the specific substrate for caspase-3/7 Ac-DEVD-AFC. Each value is expressed as change in fluorescence as a function of time ($\Delta F/\Delta t$) and is expressed relative to control cells. Values are means ± SD of four independent experiments, each performed in duplicate. *$P < 0.05$

Fig. 8. The mechanism of cathepsin X involvement in neuroinflammation-induced neurodegeneration. LPS activates microglia by triggering several signaling pathways and secreting inflammatory cytokines and certain cathepsins such as cathepsin X. Cathepsin X inhibitor AMS36 slows down these processes and ameliorates LPS-mediated neuroinflammation leading to reduced neuronal death and apoptosis. Additionally, AMS36 reverses the decrease in level of microglia-secreted active γ-enolase, thus contributing to neuroprotection.

Figure legends for Supplementary material

Fig. S1. Secondary antibody control staining. (A-B) Representative images of double immunofluorescence staining with anti-mouse Alexa Fluor-488 (green fluorescence) and anti-goat Alexa Fluor-555 (red fluorescence) secondary antibodies **(A)** and with anti-rabbit Alexa Fluor-488 (green fluorescence) and anti-goat Alexa Fluor-555 (red fluorescence) secondary antibodies **(B)** in unstimulated BV2 cells (control) and cells stimulated with LPS (1 µg/ml) for 24 h. *Scale bars* 20 µm.

Fig. S2. Effect of LPS stimulation on cathepsin X expression and activity in EOC 13.31 cells. EOC 13.31 cells were stimulated with the increasing concentrations of LPS (0.5 - 2 µg/ml) for 24 h or the time period indicated. **(A)** Determination of nitrite concentration in the culture supernatants of LPS stimulated EOC 13.31 cells. Values are means ± SD of five independent experiments. $^*P < 0.05$ **(B)** The levels of cathepsin X in cell lysates and culture supernatants of EOC 13.31 cells stimulated with various concentrations of LPS (0.5 - 2 µg/ml) for 24 h were measured by ELISA, using goat anti-cathepsin X AF934 and mouse anti-cathepsin X 3B10 as a capture and detection antibody, respectively. Values are means ± SD of three independent experiments. $^*P < 0.05$ **(C)** Cathepsin X activity in cell lysates and culture supernatants were determined at various concentrations of LPS (0.5 -2 µg/ml) for 24 h, using cathepsin X-specific substrate Abz-Phe-Glu-Lys(Dnp)-OH. Values are means ± SD of five independent experiments. $^*P < 0.05$

Fig. S3. Expression of γ-enolase in LPS-stimulated EOC 13.31 cells. Cells were stimulated with the increasing concentrations of LPS (0.5 - 2 µg/ml) in the absence or presence of cathespin X inhibitor AMS36 (10 µM) for 24 h. **(A)** The levels of active γ-enolase in cell lysates and culture supernatants of EOC 13.31 cells stimulated with LPS for 24 h were measured by ELISA, using for capture mouse antibody against C-terminal γ-enolase, suitable for detecting its active form. Values are means ± SD of three independent experiments. $^*P < 0.05$ **(B)** The levels

of active γ-enolase in culture supernatants of EOC 13.31 cells pretreated with AMS36 for 1 h prior to LPS stimulation for 24 h were measured by ELISA. Values are means ± SD of three independent experiments. *$P < 0.05$

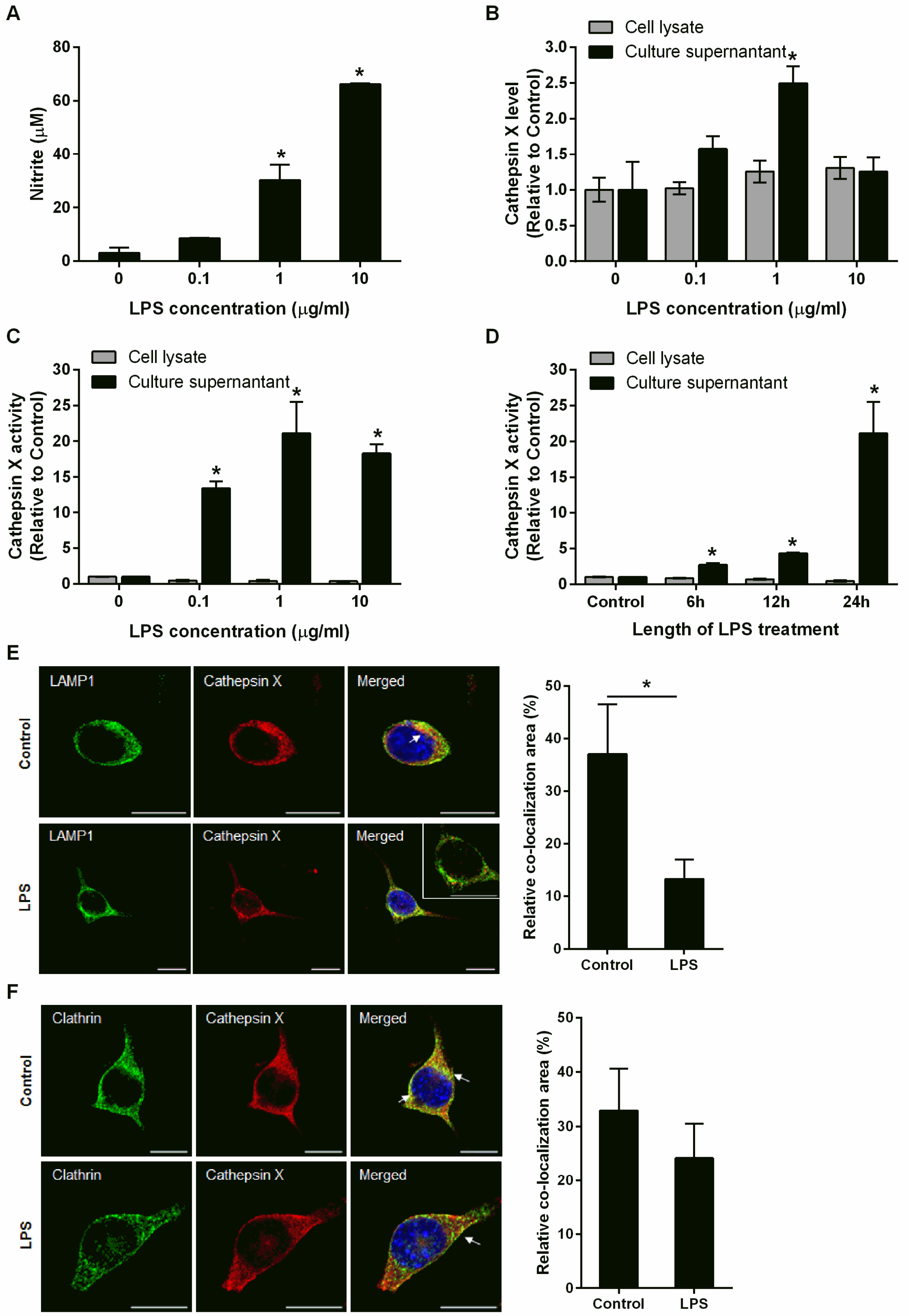
A
Nitrite (μM)
80
60
40
20
0
*
*
0
0.1
1
10
LPS concentration (μg/ml)
B
Cell lysate
Culture supernatant
Cathepsin X level (Relative to Control)
3.0
2.5
2.0
1.5
1.0
0.5
0.0
*
0
0.1
1
10
LPS concentration (μg/ml)
C
Cell lysate
Culture supernatant
Cathepsin X activity (Relative to Control)
30
25
20
15
10
5
0
*
*
*
0
0.1
1
10
LPS concentration (μg/ml)
D
Cell lysate
Culture supernatant
Cathepsin X activity (Relative to Control)
30
25
20
15
10
5
0
*
*
*
Control
6h
12h
24h
Length of LPS treatment
E
Control
LPS
LAMP1
Cathepsin X
Merged
Relative co-localization area (%)
50
40
30
20
10
0
*
Control
LPS
F
Control
LPS
Clathrin
Cathepsin X
Merged
Relative co-localization area (%)
50
40
30
20
10
0
Control
LPS

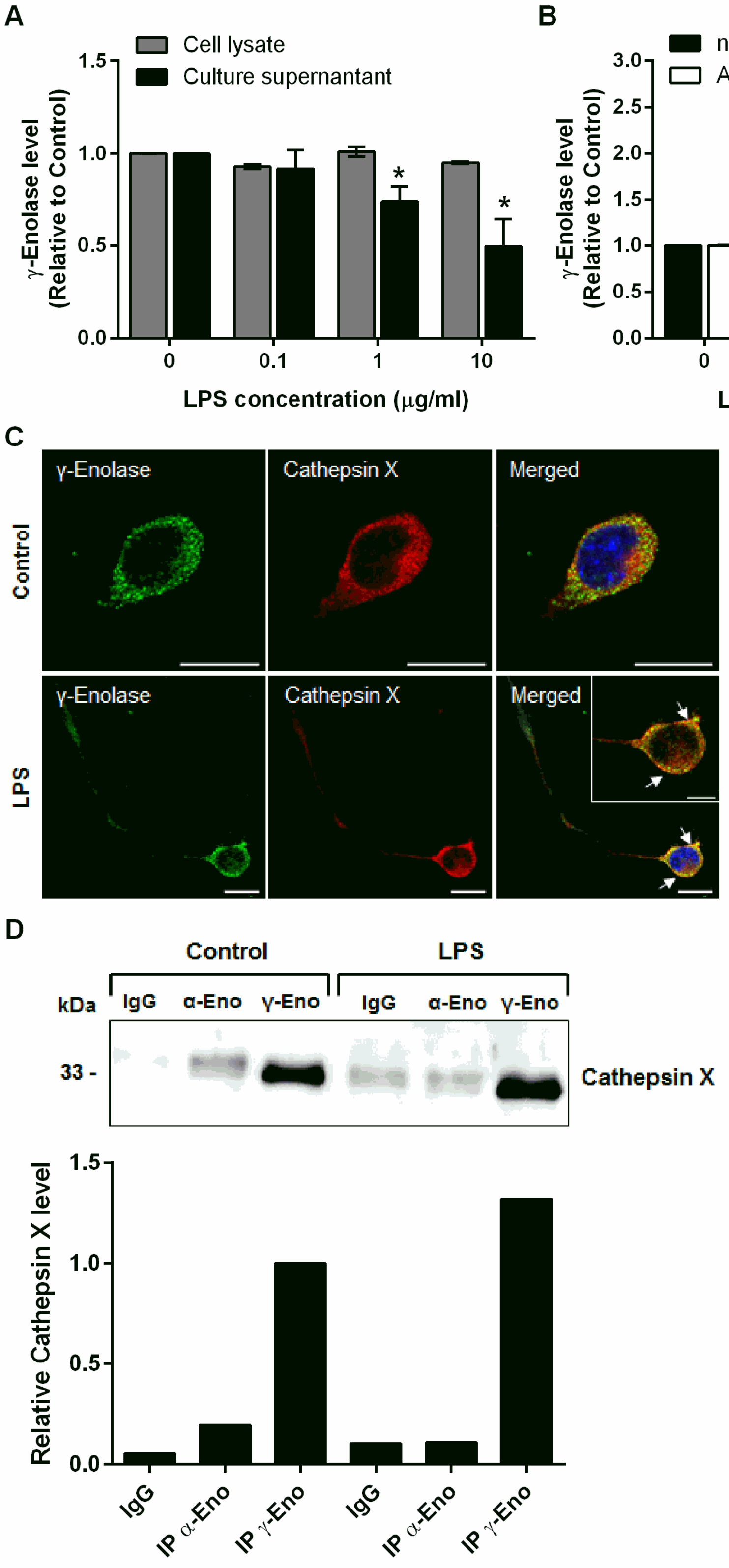
A
Cell lysate
Culture supernantant
γ-Enolase level (Relative to Control)
1.5
1.0
0.5
0.0
*
*
0
0.1
1
10
LPS concentration (μg/ml)
B
no inhibitor
AMS36
γ-Enolase level (Relative to Control)
3.0
2.5
2.0
1.5
1.0
0.5
0.0
*
*
0
0.1
1
10
LPS concentration (μg/ml)
C
Control
LPS
γ-Enolase
Cathepsin X
Merged
γ-Enolase
Cathepsin X
Merged
Relative co-localization area (%)
60
40
20
0
*
Control
LPS
D
Control
LPS
kDa
IgG
α-Eno
γ-Eno
IgG
α-Eno
γ-Eno
33 -
Cathepsin X
Relative Cathepsin X level
1.5
1.0
0.5
0.0
IgG
IP α-Eno
IP γ-Eno
IgG
IP α-Eno
IP γ-Eno

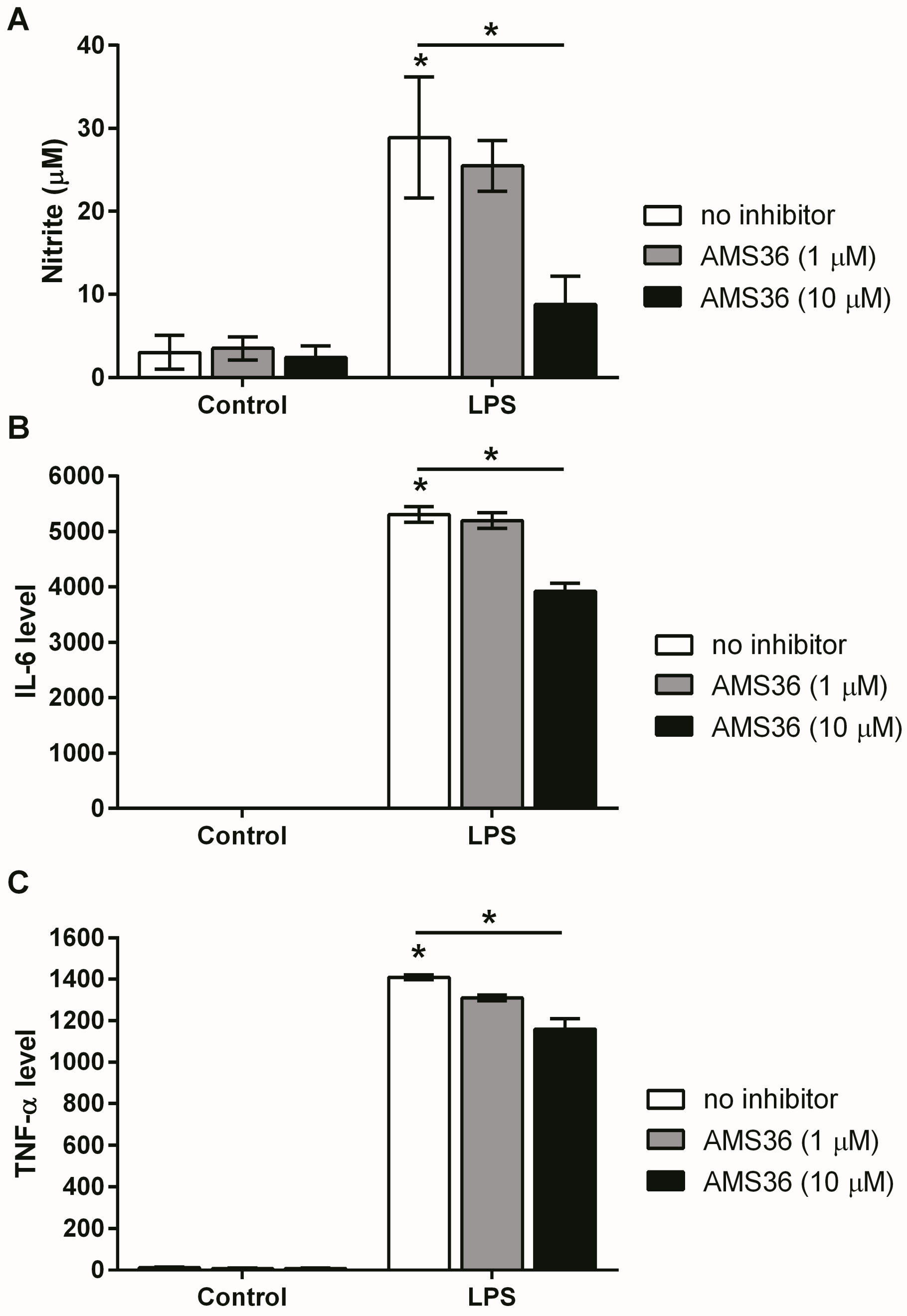
A
Nitrite (μM)
40
30
20
10
0
*
*
Control
LPS
no inhibitor
AMS36 (1 μM)
AMS36 (10 μM)
B
IL-6 level
6000
5000
4000
3000
2000
1000
0
*
*
Control
LPS
no inhibitor
AMS36 (1 μM)
AMS36 (10 μM)
C
TNF-α level
1600
1400
1200
1000
800
600
400
200
0
*
*
Control
LPS
no inhibitor
AMS36 (1 μM)
AMS36 (10 μM)

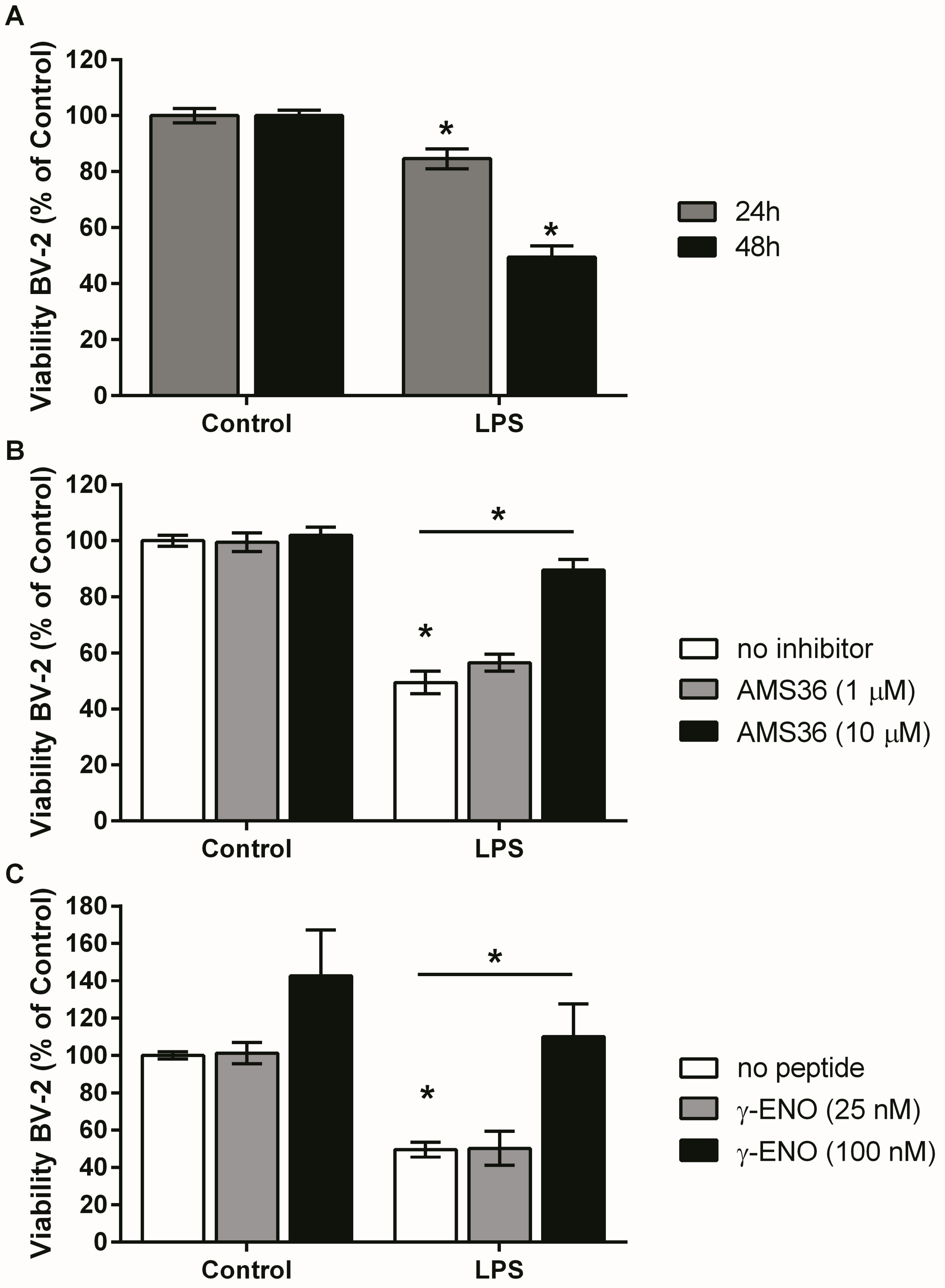
A
Viability BV-2 (% of Control)
120
100
80
60
40
20
0
*
*
Control
LPS
24h
48h
B
Viability BV-2 (% of Control)
120
100
80
60
40
20
0
*
*
Control
LPS
no inhibitor
AMS36 (1 μM)
AMS36 (10 μM)
C
Viability BV-2 (% of Control)
180
160
140
120
100
80
60
40
20
0
*
*
Control
LPS
no peptide
γ-ENO (25 nM)
γ-ENO (100 nM)

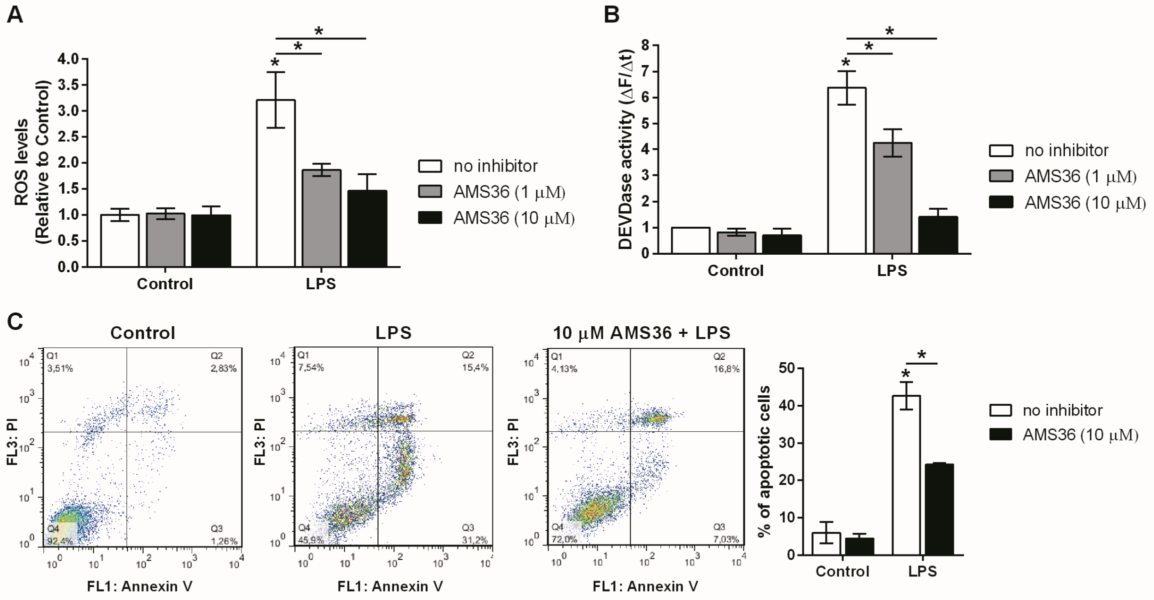
A
ROS levels
(Relative to Control)
4.0
3.5
3.0
2.5
2.0
1.5
1.0
0.5
0.0
Control
LPS
*
*
*
no inhibitor
AMS36 (1 μM)
AMS36 (10 μM)
B
DEVDase activity (ΔF/Δt)
8
7
6
5
4
3
2
1
0
Control
LPS
*
*
*
no inhibitor
AMS36 (1 μM)
AMS36 (10 μM)
C
Control
LPS
10 μM AMS36 + LPS
FL3: PI
FL1: Annexin V
Q1 3,51%
Q2 2,83%
Q3 1,26%
Q4 92,4%
Q1 7,54%
Q2 15,4%
Q3 31,2%
Q4 45,9%
Q1 4,13%
Q2 16,8%
Q3 7,03%
Q4 72,0%
10^0
10^1
10^2
10^3
10^4
% of apoptotic cells
50
40
30
20
10
0
Control
LPS
*
*
no inhibitor
AMS36 (10 μM)

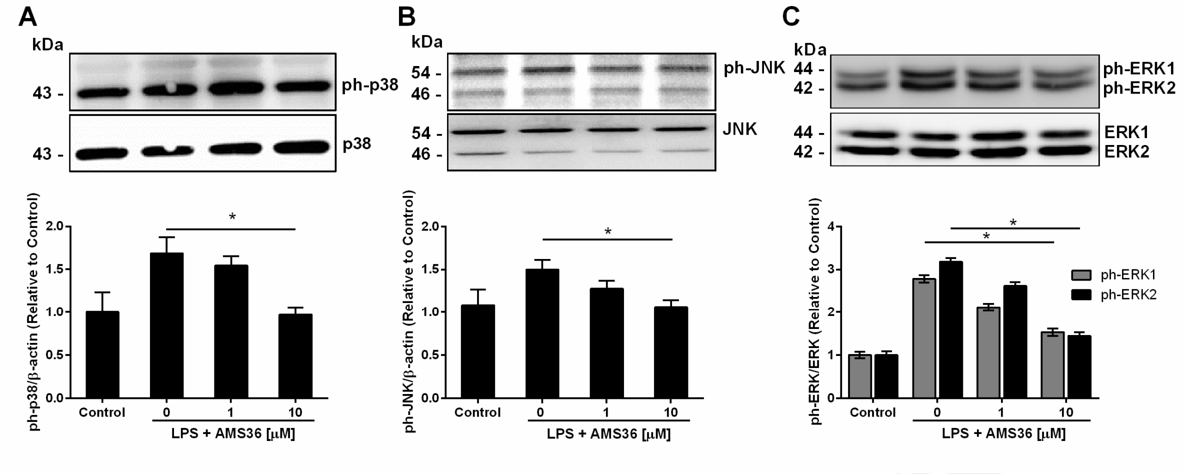
A
kDa
43 -
ph-p38
43 -
p38
ph-p38/β-actin (Relative to Control)
2.0
1.5
1.0
0.5
0.0
*
Control
0
1
10
LPS + AMS36 [μM]
B
kDa
54 -
46 -
ph-JNK
54 -
46 -
JNK
ph-JNK/β-actin (Relative to Control)
2.0
1.5
1.0
0.5
0.0
*
Control
0
1
10
LPS + AMS36 [μM]
C
kDa
44 -
42 -
ph-ERK1
ph-ERK2
44 -
42 -
ERK1
ERK2
ph-ERK/ERK (Relative to Control)
4
3
2
1
0
*
*
ph-ERK1
ph-ERK2
Control
0
1
10
LPS + AMS36 [μM]

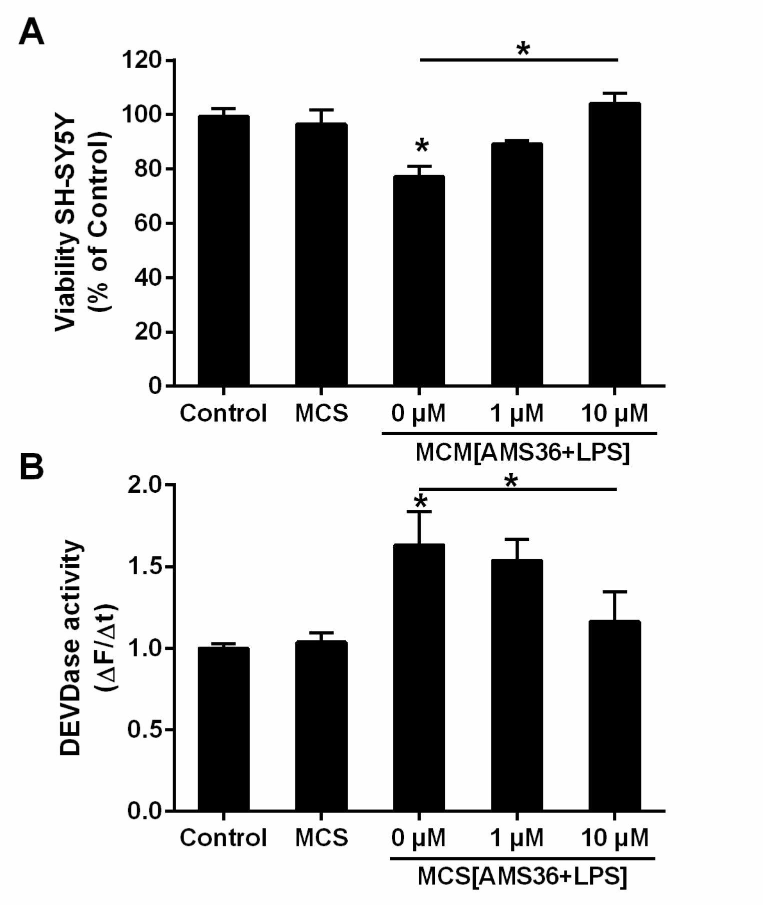
A
Viability SH-SY5Y (% of Control)
0
20
40
60
80
100
120
*
*
Control
MCS
0 μM
1 μM
10 μM
MCM[AMS36+LPS]
B
DEVDase activity (ΔF/Δt)
0.0
0.5
1.0
1.5
2.0
*
*
Control
MCS
0 μM
1 μM
10 μM
MCS[AMS36+LPS]

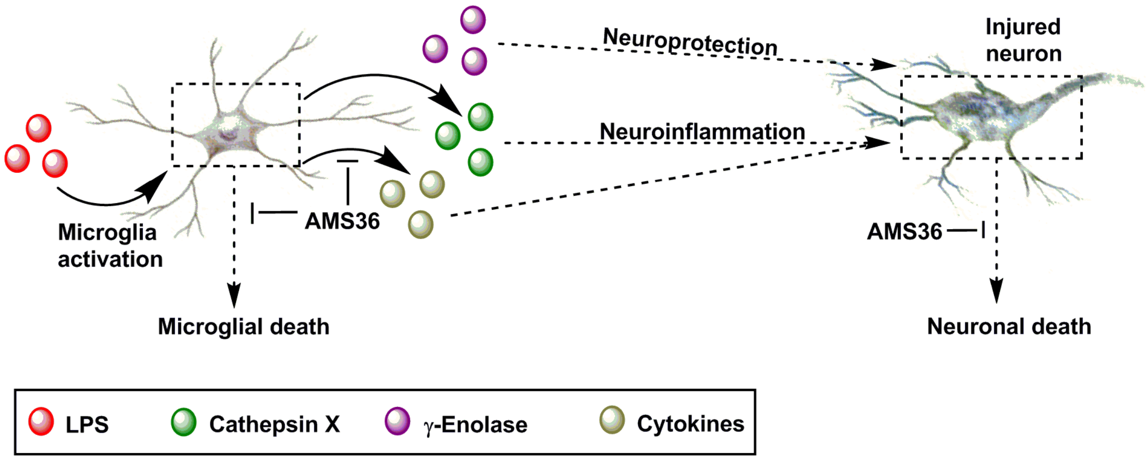
Neuroprotection
Injured
neuron
Neuroinflammation
Microglia
activation
AMS36
AMS36
Microglial death
Neuronal death
LPS
Cathepsin X
γ-Enolase
Cytokines

Inhibition of cathepsin X reduces the strength of microglial-mediated neuroinflammation

Anja Pišlar[a,*], Biljana Božić[b], Nace Zidar[c] and Janko Kos[a,d]

Highlights

- i.) *Microglia activation induces cathepsin X expression and its activity.*
- ii.) *Cathepsin X inhibition suppresses microglia activation.*
- iii.) *Cathepsin X mediates microglia activation-mediated neurodegeneration.*
- iv.) *Cathepsin X inhibition exerts neuroprotection.*